



Thermodynamic signatures of fragment binding: Validation of direct versus displacement ITC titrations



Eggert Rühmann^a, Michael Betz^a, Marie Fricke^b, Andreas Heine^a, Martina Schäfer^b, Gerhard Klebe^a

^a Institute of Pharmaceutical Chemistry, Philipps-University Marburg, Marbacher Weg 6, 35037 Marburg, Germany

^b Bayer HealthCare, Müllerstr. 178, 13353 Berlin, Germany

ARTICLE INFO

Article history:

Received 22 September 2014

Received in revised form 20 November 2014

Accepted 4 December 2014

Available online 16 December 2014

Keywords:

Thermodynamic signature
Isothermal titration calorimetry
Protein–fragment binding
Displacement titrations
Low-*c* value titration
Thrombin

ABSTRACT

Background: Detailed characterization of the thermodynamic signature of weak binding fragments to proteins is essential to support the decision making process which fragments to take further for the hit-to-lead optimization. **Method:** Isothermal titration calorimetry (ITC) is the method of choice to record thermodynamic data, however, weak binding ligands such as fragments require the development of meaningful and reliable measuring protocols as usually sigmoidal titration curves are hardly possible to record due to limited solubility.

Results: Fragments can be titrated either directly under low *c*-value conditions (no sigmoidal curve) or indirectly by use of a strong binding ligand displacing the pre-incubated weak fragment from the protein. The determination of Gibbs free energy is reliable and rather independent of the applied titration protocol.

Conclusion: Even though the displacement method achieves higher accuracy, the obtained enthalpy–entropy profile depends on the properties of the used displacement ligand. The relative enthalpy differences across different displacement experiments reveal a constant signature and can serve as a thermodynamic fingerprint for fragments. Low *c*-value titrations are only reliable if the final concentration of the fragment in the sample cell exceeds 2–10 fold its *K_D* value. Limited solubility often prevents this strategy.

General significance: The present study suggests an applicable protocol to characterize the thermodynamic signature of protein–fragment binding. It shows however, that such measurements are limited by protein and fragment solubility. Deviating profiles obtained by use of different displacement ligands indicate that changes in the solvation pattern and protein dynamics most likely take influence on the resulting overall binding signature.

© 2014 Elsevier B.V. All rights reserved.

1. Introduction

Consideration of thermodynamic binding profiles beyond sole affinity appreciations in drug optimization is increasingly regarded as a valuable analytical tool [1–3]. Analyses of thermodynamic signatures of ligand binding have shown that on late-stage optimization improved binding is frequently achieved by enhancing the entropic component to the Gibbs free energy of binding [4,5]. This results either from an appropriate rigidification of the lead scaffold in the protein-bound conformation, or from the attachment of lipophilic groups of growing size to optimally fill remaining unoccupied pockets in the binding site. Usually these strategies make the lead candidates more complex and overall more ‘greasy’, provoking concomitant problems such as unsatisfactory bioavailability or growing risk of undesired toxicity [6–8]. Accordingly, the hypothesis has been proposed to start lead optimization with small enthalpically advantaged binders as the entropic component will be added inevitably to the binding signature during late-stage optimization [9,10]. Therefore, methods giving reliable access to thermodynamic signature analysis, particularly of weak binding initial hits, are essential to support the decision making process which compounds to take further for lead optimization. To this end, more

meaningful measuring protocols to record accurate isothermal titration calorimetry (ITC) data of two-digit micromolar to even millimolar binders are required.

Anticipating a sufficiently large enthalpic binding component, the scope of ITC measurements to record protein–ligand complex formation ranges approximately from low-micromolar to two-digit nanomolar binders. In consequence weak binding ligands such as fragments are hardly detectable by this method [11–13]. To some degrees this difficulty can be overcome by titrating huge amounts of protein and fragment at very high concentrations. Nonetheless, this strategy of direct titrations is limited as usually protein supply is crucial and low solubility of either protein, and/or ligand or increasing protein degradation at high concentration impedes direct ITC titrations. Furthermore, titration curves recorded under these conditions are difficult to analyze as they usually lack sigmoidal shape and their inflection point can hardly be defined. The enthalpic binding component can only be extracted if the binding stoichiometry is arbitrarily adjusted to, e.g., 1:1 during the data fitting. However, frequently higher binding ratios are given for small binders such as fragments. In contemporary drug discovery fragment-based approaches play an increasingly important role and ITC would be an ideal complementary asset to identify the most

promising candidates with high enthalpic efficacy [1,8]. At present fragments are usually discovered by other screening methods such as surface plasmon resonance (SPR), saturation transfer difference NMR (STD-NMR) and thermal shift analysis (TSA).

To develop ITC protocols for weak binders we used a set of fragments with milli to three-digit micromolar affinities inhibiting the serine protease thrombin, to validate direct ITC titrations versus alternative titration protocols such as displacement experiments suggested by Zhang et al. [14]

To perform the required displacement experiments we used several strong binding reference ligands of deviating structural and thermodynamic profiles to evaluate the binding properties of the selected fragments. In the present study we will show that, even though the individual thermodynamic binding profiles recorded for the various fragments can be distinct, the relative differences among the fragment profiles seem to be independent of the actually selected displacement ligand. Furthermore, the approach allows estimating experimental errors and helps to validate the reliability and validity of fragment binding profiles obtained by direct ITC titrations.

2. Results

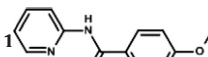
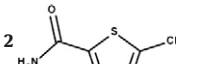
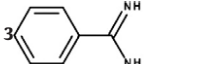
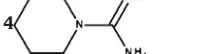
2.1. Data set of fragments and reference ligands

For the anticipated analysis we assembled a dataset of fragments binding to the serine protease thrombin, an important drug target in the blood coagulation cascade for which in recent time drugs have been launched to the market [15]. With respect to the structural and thermodynamic characterization, this protein is well established in our laboratory and from this experience we selected a sample set of appropriate reference ligands for displacement titrations. We have chosen the fragments **1–4** (Table 1) previously described as milli to micromolar binders for thrombin [16–18].

All selected fragments bind into the S1 pocket of thrombin, as could be confirmed by X-ray crystallography. The adopted binding modes are depicted in Fig. 1 together with the structures of the larger and more potent reference ligands. The corresponding structures will be reported in a subsequent study.

To perform displacement titrations in order to characterize fragment binding (see below), appropriate reference ligands are required that exhibit an affinity in the three-digit nanomolar range, as they allow direct titrations with optimal sigmoidal shape of the titration curve. We selected three different reference ligands **A–C** (Fig. 2) with distinct thermodynamic profiles and chemical composition, to investigate the influence of the reference ligand onto the thermodynamic profiles of the displaced fragments.

Table 1
Chemical formulas of the studied fragments with their estimated binding constants in μM .

Fragment	K_i assay ^a	K_D displacement ITC	K_D direct ITC
	2430 ± 309	1582 ± 441	1003 ± 224
	431 ± 27	507 ± 139	475 ± 110
	258 ± 1	455 ± 109	355 ± 29
	111 ± 2	197 ± 74	107 ± 20

^a The estimated standard deviations have been calculated based on at least triplicate measurements

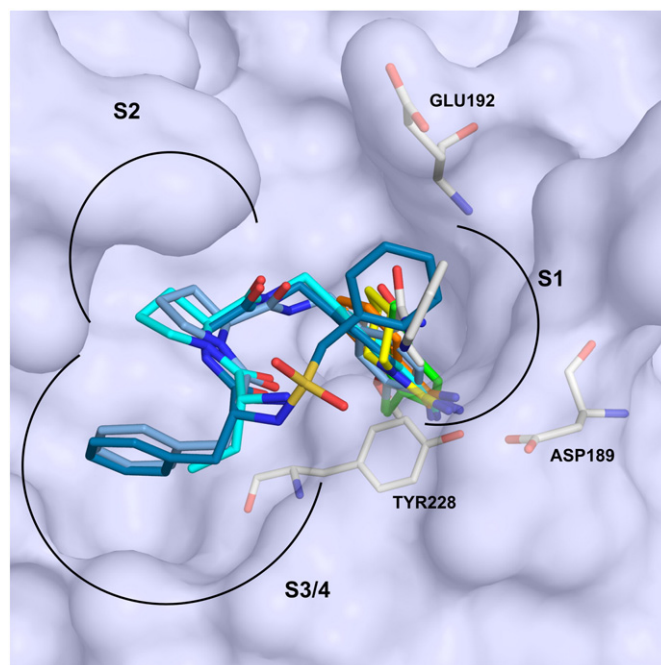


Fig. 1. Fragments **1** (white), **2** (green), **3** (orange), **4** (yellow) and reference ligands **A** (light blue), **B** (turquoise) and **C** (dark blue) bound to the active site of thrombin. The protein is indicated by its solvent-accessible surface (white) and the three residues Asp 189, Glu192 and Tyr228. Oxygen atoms are indicated in red, nitrogen atoms in blue, sulfur atoms in yellow. The specificity pockets S1, S2, S3/4 of the protease are schematically indicated.

As a first step, we characterized the reference ligands by direct titration experiments resulting in thermograms similar to that obtained for ligand **A** shown in Fig. 3a. The synthesis of the reference compounds has been described previously [19–21].

In the following we will discuss only the ΔG° and ΔH° values, as these are the properties actually determined in an ITC experiment. The entropic component, usually specified as $-\Delta S^\circ$, is calculated as the numerical difference of Gibbs free energy and enthalpic binding contribution according to $\Delta G^\circ = \Delta H^\circ - T\Delta S^\circ$. All three reference ligands have been assessed with respect to a possibly superimposed protonation change which can be discovered by performing the titration experiments from different buffer conditions.

The compound classes of ligands **A** and **B** have been studied in great detail in the past and a simultaneous compensatory proton entrapment and release has been recognized suggesting a release of about 0.5 mol protons upon ligand binding from His57 which is partially protonated in the uncomplexed state. Virtually the same amount is picked up by the ligand upon protein binding [21]. For a scaffold closely related to that of ligand **C** previous studies indicated no compensatory protonation effect to be superimposed onto the binding event [19,22]. Nonetheless, to minimize possibly sophisticated effects from proton release or pick-up of the surrounding buffer, all experiments were performed in pyrophosphate buffer which shows nearly negligible heat effects for changes in protonation states. Reference ligand **A** ($K_D = 269 \pm 50$ nM; $\Delta G^\circ = -37.5 \pm 0.5$ kJ/mol) exhibits a predominantly enthalpic binding signature ($\Delta H^\circ = -45.1 \pm 0.8$ kJ/mol) and addresses the S1 pocket of thrombin with a dichloro benzyl moiety, the S2 pocket with a proline and the S3 pocket with a D-Phe residue (Fig. 1 and Fig. 2). Reference ligand **B** ($K_D = 110 \pm 16$ nM; $\Delta G^\circ = -39.7 \pm 0.4$ kJ/mol) is a less enthalpic binder ($\Delta H^\circ = -28.8 \pm 0.8$ kJ/mol) and accommodates the S1 pocket of thrombin with a benzamidine moiety, the S2 pocket with a proline and the S3 pocket with a homo-Ala residue. Reference ligand **C** ($K_D = 162 \pm 34$ nM; $\Delta G^\circ = -38.8 \pm 0.6$ kJ/mol) shows

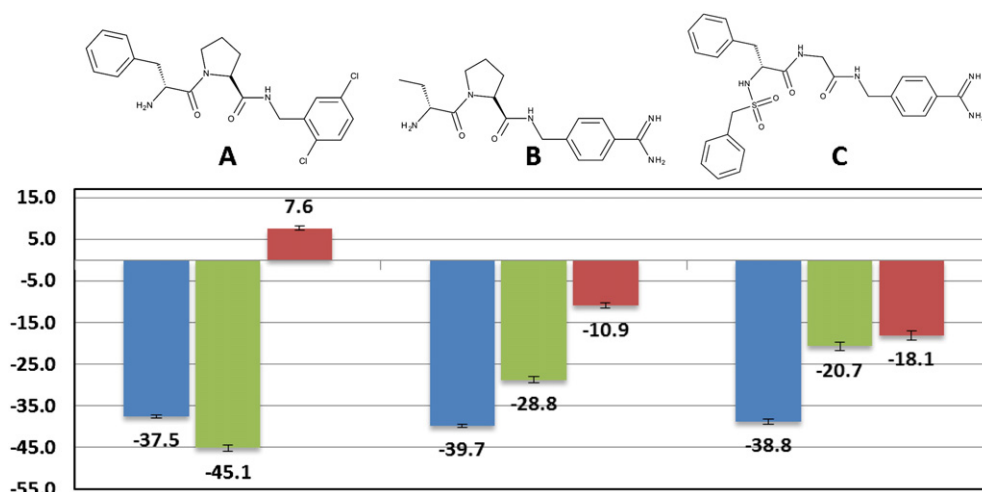


Fig. 2. Thermodynamic parameters (ΔG° in blue, ΔH° in green, $-T\Delta S^\circ$ in red in kJ/mol) determined by direct ITC titrations for the strong binding reference ligands **A**, **B** and **C**. The estimated standard deviations, calculated from at least triplicate measurements, are indicated by the black error bars.

balanced enthalpic ($\Delta H^\circ = -20.7 \pm 0.9$ kJ/mol) and entropic ($-T\Delta S^\circ = -18.1 \pm 1.1$ kJ/mol) binding contributions and is accommodated in the S1 pocket of thrombin using its benzamidine moiety, in the S2 pocket by an Ala residue, and the S3 pocket is occupied by a D-Phe residue and the S4 pocket by a benzylsulfonamide group.

2.2. Importance of the *c*-value for the shape of the titration curve

Crucial for the shape of a recorded ITC titration curve is the so-called *c* parameter, first introduced by Wiseman [23] and discussed in detail by Turnbull et al. [24]. Detailed parameter studies have elucidated that a *c*-value of ≥ 10 reveals a proper sigmoidal curve but the value should remain below 1000 to avoid a vertical stepwise curve. However, if *c* falls below 10, the inflection point can hardly be extracted as the titration curve is no longer sigmoidal. In consequence, the binding stoichiometry is no longer available from the experiment without arbitrary assumptions. An example for such a titration curve is given in Fig. 3b.

The following estimation of the concentrations required for an ITC experiment with fragments should make the practicability of such a determination clearer. To obtain a minimal *c*-value of 10 for a typical fragment with $K_D = 1$ mM, a protein concentration of 10 mM in the sample cell according to $c = n[\text{Protein}] K$ is required. At the end of the titration the final fragment concentration should be at least twice (or even better 10-times) as high as this value to achieve sufficient saturation (s. below).

If the fragment is released from the syringe of an ITC200 device with a volume of approximately 40 μl into the sample cell which has a five-time larger volume, the concentration of the fragment in the syringe has to be at least 100 mM. In many cases, such a high solubility is difficult to achieve. Titration experiments can principally be reversed, but as a similar amount of protein will be required, solubility and particularly protein stability will hardly be accomplishable to perform such titration experiments. This crude estimation makes it obvious that protein and ligand solubilities will be the predominant limiting factors to study low-affinity systems following the popular strategy to design an ITC experiment resulting in sigmoidal titration curves.

If fragment titrations at *c*-values ≥ 10 are hardly feasible, the following alternatives can be suggested.

The first strategy focuses on displacement titrations. In this alternative, the protein must be saturated with the fragment prior to the titration experiment while preparing the protein solution. To achieve a reasonable saturation a crude estimate about the expected affinity

of the fragment must be available (see below). Subsequently, the pre-incubated weak binding ligand is displaced in a titration experiment with a beforehand characterized reference ligand. By subtracting the measured binding enthalpies of the directly titrated reference ligand and the data recorded in the displacement experiment, the thermodynamic profile of the weak binding fragment can be assessed (Fig. 3a and c). Is this protocol of any advantage with respect to the required concentrations during the experiment? The fragment which is initially dissolved in DMSO is added to the protein solution in a way to match the finally desired DMSO concentration in the sample cell and the injection syringe. Following this strategy, overall a lower concentration of the respective fragment will be needed usually not exceeding the solubility limits. The displacement titration strategy might suffer from the fact that particularly in a novel drug discovery project potent and well-characterized reference ligands for the displacement strategy are not available. However, in some drug discovery projects a potent natural product or endogenous ligand, not really suited as a lead candidate, is available that can serve as reasonable reference ligand for displacement experiments.

In case, even such a reference is missing, the only feasible alternative is to perform ITC experiments as low *c*-value titrations. As mentioned, they suffer from the fact that a sigmoidal shape is no longer given and the inflection point of the curve is poorly defined. Therefore, it is necessary to arbitrarily adjust the binding stoichiometry to a predefined value during curve fitting (Fig. 3b) and it is crucial to control concentrations of ligand and protein very accurately. To achieve a sufficient saturation of the protein with the fragment during the titration, the final concentration of the fragment added to the sample cell must be larger than its estimated K_D value. Furthermore, a reasonable binding stoichiometry, mostly set to 1:1, of the formed protein–fragment complex must be anticipated. Nonetheless, in protein crystallography often the binding of more than one fragment molecule to the target protein is observed, particularly at high concentrations, which makes the assumption of a 1:1 ratio questionable. To perform a direct low *c*-value titration of a fragment, a rather concentrated fragment solution is released from the syringe to the protein in the sample cell, however, this solution will be less concentrated than that in a scenario with a *c*-value ≥ 10 . Nonetheless, compared to the alternative displacement strategy, the required concentration even for the just described direct low *c*-value titration will be undoubtedly higher, which makes the displacement strategy better applicable under practical conditions. This aspect has also been discussed by Turnbull et al. [25,26]. To contrast the different strategy options, we will compare in the following the results obtained by displacement protocols with those recorded under direct low *c*-value conditions.

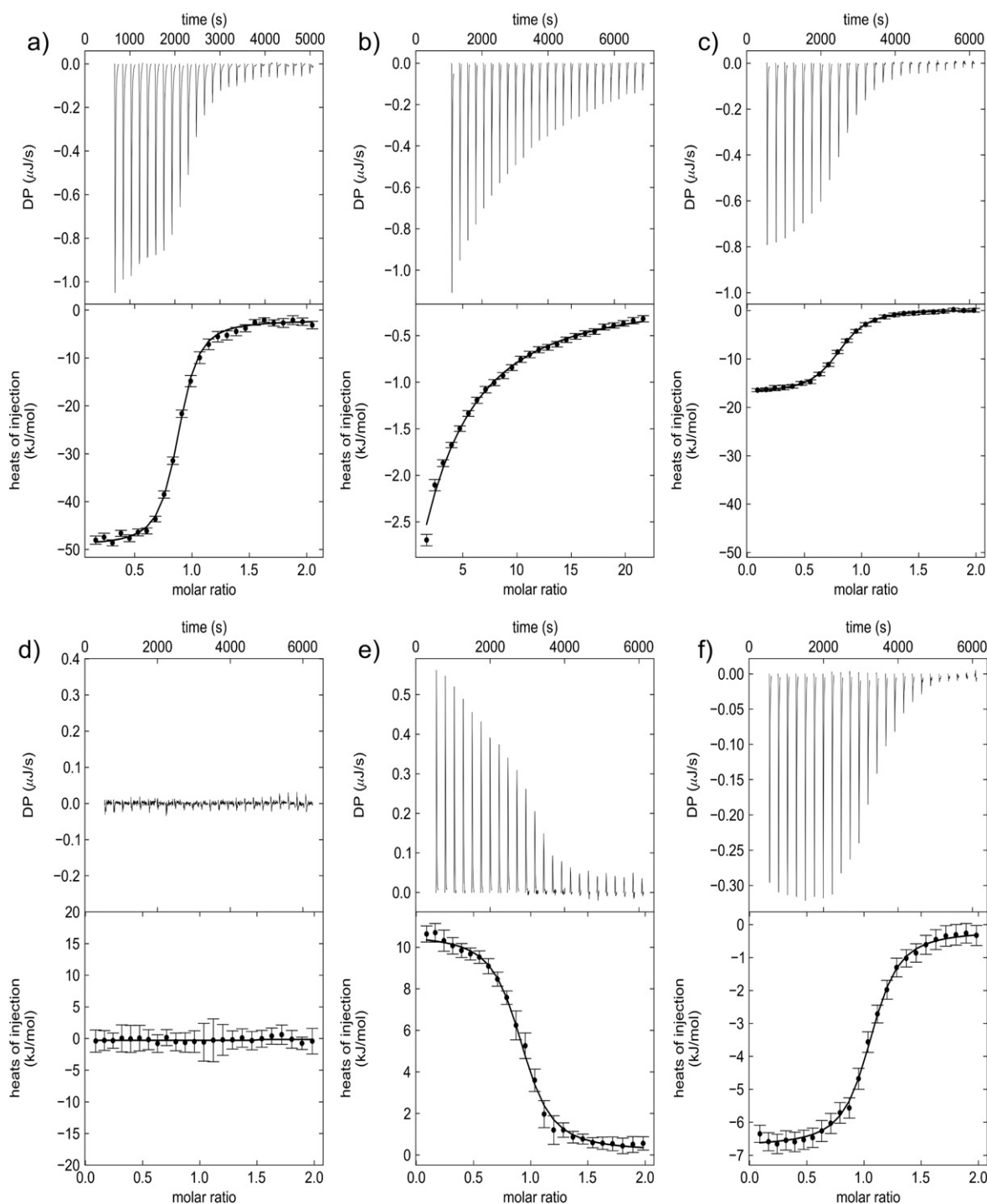


Fig. 3. Images of representative thermograms obtained by different titration protocols applied in this study. The individual titration curves show: a) reference ligand **A** in direct titration; b) fragment **2** in direct titration; c) **2** is displaced by **A**; d) **4** is displaced by **C** but no difference in binding enthalpy could be recorded; e) **2** displaced by **C**; f) **3** displaced by **C**. In all cases the heat signals (in $\mu\text{J/s}$) as a response by the release of the ligand into the protein solution is shown over the course of the experiment along with the integrated heat signals of the injections (kJ/mol).

2.3. Estimation of fragment affinity

Both suggested ITC protocols require a crude estimation of the binding constant of the studied fragment to secure sufficient saturation of the protein at the end of the titration. In a real-life scenario, K_i values of the studied fragments are not necessarily available. However, in the present case, they could be determined by an independent, highly sensitive fluorescence-based assay (see Section 5 Experimental section/materials & methods).

2.4. Results obtained by the displacement titrations

The reference ligands appropriate for displacement titrations need to exhibit an affinity in three-digit nanomolar range (optimal 100 to 400 nM) to fall into the optimal sensitivity range of ITC. This allows thermodynamic characterization via direct titrations with good c -values of 20–100 and a low standard deviation for K_D and ΔH° . Broecker et al. suggested a c -value of 40 to be optimal [27].

In Fig. 4a), b), and c), the results for the displacement titrations of fragments **1–4** using the reference ligands **A–C** are compiled.

The fragment concentrations for the pre-incubation were adjusted in a way to achieve 2 mM concentration in the sample cell. For the displacement titrations using the three reference ligands, the deviations of the Gibbs free energy determinations are rather small, suggesting a standard deviation of 0.6 kJ/mol. This fact emphasizes ITC as an ideal method to determine reliable dissociation constants. In contrast, facing the individual experiments based on different reference ligands against one another, the recorded enthalpies show mutual deviations which are much larger than the expected experimental error even considering the fact that two subsequent titration experiments will involve, owing to error propagation, larger uncertainties in the heat signal determinations. This suggests that the use of different

reference ligands does not reveal similar enthalpies to displace the considered pre-incubated fragments.

2.5. Results obtained by direct low *c*-value titrations

In all experiments a concentrated fragment solution was titrated to the protein in the sample cell. For **1** and **2** an almost saturated solution of 5 mM has been applied. Owing to their better solubility, fragments **3** and **4** could be titrated from the syringe with a concentration of 10 mM. The obtained thermodynamic profiles are shown in Fig. 4d. Remarkably, the binding free energies for the direct titrations match reasonably well with those obtained by the displacement titrations. The enthalpic signal of **1**, which is affected by rather large standard deviations, falls roughly (within the error bars) into the range indicated by the three

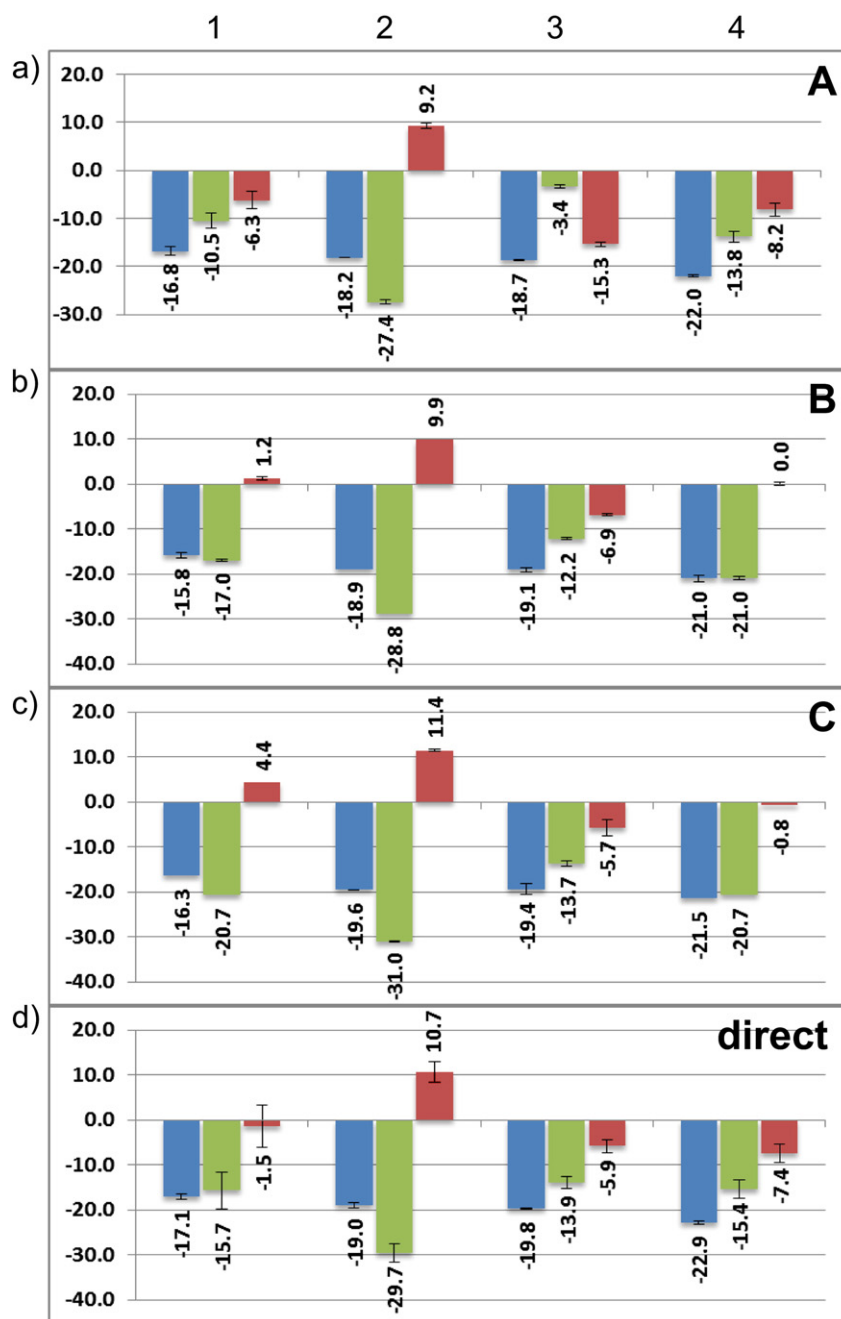


Fig. 4. Thermodynamic signatures (ΔG° in blue, ΔH° in green, $-\Delta S^\circ$ in red, all data in kJ/mol) for fragments **1–4** determined by ITC displacement titrations using reference ligands **A** (a), **B** (b), **C** (c) and obtained by direct low-*c* ITC titrations (d) are shown. The estimated standard deviations from at least triplicate measurements of the different experiments are indicated by the black error bars. In case the enthalpies were taken as similar to the binding enthalpy of the reference ligand (B-2, C-1 and C-4) no error estimations are indicated.

displacement titrations. For **2–4** the enthalpic signals could be determined with lower standard deviations. Interestingly enough, they match, depending on the used reference ligand, in some cases quite well with the values found by the displacement experiments. In other cases significant deviations are observed. These results suggest furthermore, that the profiles obtained for the different ligands depend on the chosen reference ligand.

For low *c*-value titrations the final concentration of the fragment in the sample cell is crucial and has to exceed its binding constant. To study the influence of the attained fragment concentration at the end of the titration, we determined the thermodynamic parameters for **4** using different concentrations in the syringe. The results are listed in Table 2 and the corresponding thermograms are shown in Fig. 5. The stoichiometric equivalence, adjusted in the evaluation procedure, is passed, dependent on the concentration, after a deviating number of injections released from the syringe to the sample cell. By use of the lowest syringe concentration of 1 mM, we observe a higher binding affinity for **4** compared to the other three concentrations (5 mM; 10 mM and 15 mM) which show, among each other, rather consistent values. Nonetheless, with increasing concentrations in the syringe, larger standard deviations of ΔH° are recorded.

3. Discussion

The different ITC experiments show that the determination of the binding constant and accordingly of the Gibbs free energy of binding is less dependent on the selected titration strategy than the enthalpy values. In Fig. 6, the affinities based on the various K_D values determined from direct and displacement ITC experiments are plotted against the K_i values from the biochemical assay of fragments **1–4**.

A convincing correlation of $r^2 = 0.95$ is observed for the displacement ITC experiments whereas direct ITC titrations show a slightly lower correlation of $r^2 = 0.89$.

We selected three reference ligands of which **A** is a strong enthalpy-dominated binder, whereas **B** and **C** show smaller enthalpic signals. This leads to the fact that e.g., the displacement of **2** by **A** (Fig. 3c) and of **3** by **C** (Fig. 3f) results in an exothermic displacement reaction whereas the displacement of **2** by **C** corresponds to an endothermic process (Fig. 3e). For the titrations of **B** to displace **2**, **C** to displace **1** and **C** to displace **4** no significant enthalpy difference signals could be recorded (e.g. Fig. 3d), simply as the signal for the release of the pre-incubated fragment from the protein is enthalpically compensated by the binding of the more potent reference ligand. For these fragments the binding enthalpies were supposed to match the binding enthalpy of the respective reference ligands (ΔH° of **C** for **C** displacing **1** and **4**; ΔH° of **B** for **B** displacing **2**) and we refrained from giving error estimations for these titrations (Fig. 4). Instead of estimating roughly the accuracy we consider the errors found for the characterization of the reference ligands, which, however, will likely underestimate the actually given uncertainties of the measurements. Presumably, the direct titrations of the strong binding ligands can be determined more accurately and the influence of error propagation due to two subsequent titration experiments is underrated in the current evaluation and error assignment.

In case of the flat thermograms, we calculated the free energy of ΔG° of the fragment as the mean of the ΔG° values obtained by the titrations

with the other two reference ligands which produced a measurable enthalpic signal. In Fig. 7 we compiled the relative differences in the binding enthalpies of the various fragments and the reference ligands. This diagram clearly shows that, different to the ΔG° determinations, the recorded enthalpy signals strongly depend on the profile of the selected reference ligand.

To emphasize the dependence on the profiles of the applied reference ligands, we plotted the binding enthalpy determined for the fragments in the individual displacement experiments and also from the direct low *c* titration experiment (Fig. 8).

Interestingly, this evaluation reveals a similar relative difference of each fragment independent of the actually applied displacement ligands. For example, fragment **1** binds much less enthalpic than fragment **2** or fragment **4** is a more enthalpic binder than **3**. According to this evaluation, fragment **2** is the most enthalpic binder of the series. Fragment **1** shows less enthalpic binding compared to **2** and **4**, however on average, a slightly more exothermic signature is apparent compared to **3**.

As an alternative scenario ITC experiments can be performed as low *c*-value titrations. The disadvantage of this strategy is the fact that the inflection point of the titration curve is poorly defined and the binding stoichiometry must be fixed arbitrarily. To achieve a sufficient saturation of the titrated protein, the concentration of the added fragment to the sample cell must be larger than its K_D value, simultaneously assuming a particular binding stoichiometry, e.g., of 1:1 for the formed protein–fragment complex. Turnbull et al. experienced comparable results for titrations where only 70, 80 or 90% protein saturation could be achieved which indicates some robustness of the titration settings [24,26]. Errors in the determination of K_D at very low *c*-values are becoming larger with decreasing amount of protein saturation as investigated by Tellinghuisen [28]. For example the determination of the binding of an affinity constant achieving only 50% saturation shows a 4-fold higher error compared to the measurement performed at a concentration of 93% saturation.

In our direct low *c*-value titrations, for fragment **1** we could only accomplish a final concentration in the sample cell of about 1 mM (which corresponds to approx. 30% protein saturation) due to its poor solubility in the applied buffer. In the biochemical assay we determined a K_i value of 2.4 mM and in the displacement titrations a K_D value of 1.6 mM, respectively. Based on the K_i value, we can estimate as end point of our titration approximately a 30% saturation of the protein, accordingly the required excess concentration of the fragment has not been realized. As a matter of fact, the direct low *c*-value titration results in rather large errors of the binding enthalpy determination (Fig. 4d). In consequence, the ΔH° values obtained by this direct low *c*-value titration compared to those determined by the displacement titrations show largely deviating values (direct $\Delta H^\circ = -15.7 \pm 4.1$ kJ/mol; **A** $\Delta H^\circ = -10.5 \pm 1.6$ kJ/mol; **B** $\Delta H^\circ = -17.0 \pm 0.3$ kJ/mol; **C** $\Delta H^\circ = -20.7 \pm 0.9$ kJ/mol). This observation is evidently associated with the experimental uncertainties and errors in the parameter determination.

By contrast the results obtained for the direct titration of fragment **2** agree reasonably well with the results derived from the three displacement experiments (direct $\Delta H^\circ = -29.7 \pm 2.0$ kJ/mol; **A** $\Delta H^\circ = -27.4 \pm 0.5$ kJ/mol; **B** $\Delta H^\circ = -28.8 \pm 0.8$ kJ/mol; **C** $\Delta H^\circ = -31.0 \pm 0.1$ kJ/mol) (Fig. 4). Exhibiting a binding affinity of about 500 μ M fragment **2** can easily attain the required degree of saturation of the protein of more than 70%. Also the strong enthalpic signal of $\Delta H^\circ = -29.7 \pm 2.0$ kJ/mol in the direct titration leads to good signal-to-noise ratio allowing data integration associated with lower uncertainties.

Also the direct titrations of fragment **3** ($\Delta H^\circ = -13.9 \pm 1.2$ kJ/mol) match well with the results obtained by displacement titrations with reference ligands **B** ($\Delta H^\circ = -12.2 \pm 0.3$ kJ/mol) and **C** ($\Delta H^\circ = -13.7 \pm 0.7$ kJ/mol), however, not for the titration using ligand **A** ($\Delta H^\circ = -3.7 \pm 0.3$ kJ/mol) (Fig. 4).

Table 2

Thermodynamic parameters in kJ/mol determined for **4** in direct low-*c* titrations using solutions of deviating concentrations in the syringe.

4 syringe concentrations	ΔG°	ΔH°	$-T \cdot \Delta S^\circ$
1 mM	-25.2 ± 0.2^a	-13.4 ± 0.1	-11.7 ± 0.3
5 mM	-22.8 ± 0.2	-15.4 ± 2.8	-7.4 ± 3.0
10 mM	-22.6 ± 0.2	-16.3 ± 2.8	-6.3 ± 2.5
15 mM	-22.4 ± 0.5	-14.1 ± 4.6	-8.2 ± 4.1

^a The shown uncertainties have been calculated as standard deviations resulting from duplicate measurements.

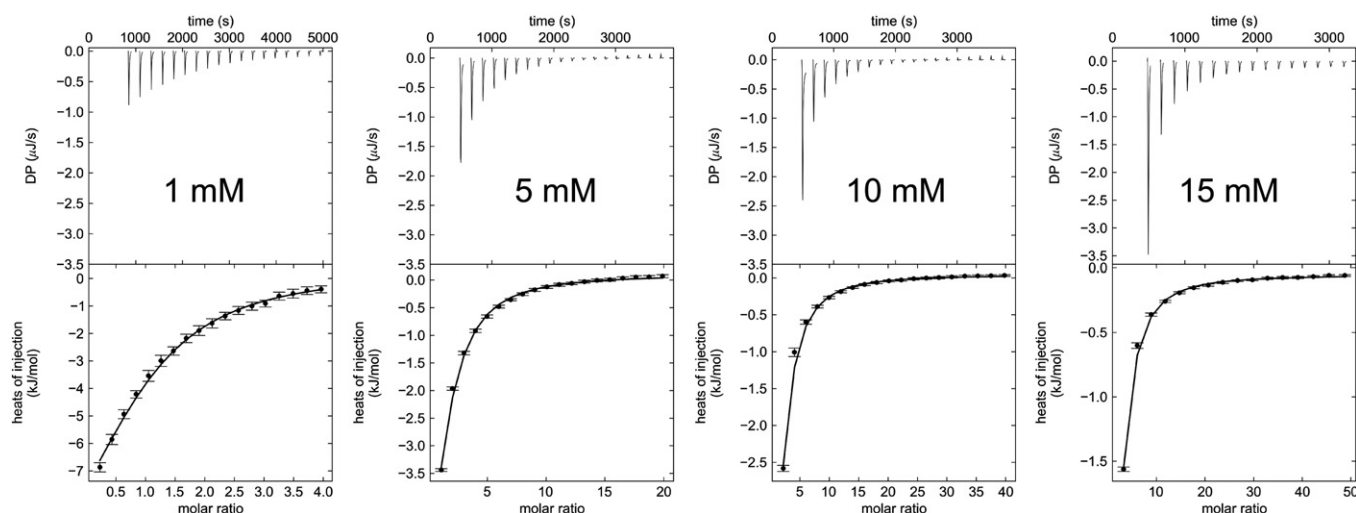


Fig. 5. Thermograms of **4**, applying different high fragment concentrations from the syringe.

It is quite remarkable that fragment **4** which appears on the first sight chemically related to fragment **3** and which should experience a similar binding mode in the S1 pocket of thrombin shows a reverse signature of the measured enthalpy values. The result of the direct titration ($\Delta H^\circ = -15.4 \pm 2.1$ kJ/mol) fits to the displacement experiment with reference ligand **A** ($\Delta H^\circ = -13.8 \pm 1.1$ kJ/mol) whereas the titrations using **B** ($\Delta H^\circ = -21.0 \pm 0.3$ kJ/mol) and **C** ($\Delta H^\circ = -21.7 \pm 0.9$ kJ/mol) as reference ligands result in quite deviating binding enthalpies. In our opinion, the observed deviations are too large to be solely explained by uncertainties of the experiments. Working under ideal conditions with highly diluted solutions and assuming additivity of all titration steps, the same enthalpic signature should result independently by which reference ligand a given fragment is displaced from the protein. However, the applied high concentrations make deviations from ideal additivity likely and it is in question whether microscopically the replacement of a given fragment by different reference ligands follows identical molecular mechanisms. Supposedly, the individual steps passed through involve cooperative changes of the solvent structure and the dynamic properties of the protein which depend on the type of reference ligand used for the individual titration experiments.

To study the influence of different syringe concentrations which lead to deviating concentrations of the fragment in the sample cell at the end of the titration, we titrated **4** at four different concentrations (Table 2, Fig. 5). At the lowest concentration of 1 mM only a saturation of the protein of about 63% is attained (see Exp. Section). As a result, ΔG° is overestimated and a too small value is found for ΔH° by integrating over all peaks. At the higher concentrations much better saturation is achieved (5 mM approx. 90%; 10 mM approx. 95% and 15 mM approx. 97%). However, higher fragment concentrations in the syringe lead to an earlier saturation of the protein usually within only 1–2 injections, therefore extrapolation of the incomplete binding isotherm becomes crucial and rather uncertain at higher concentrations. Quite large standard deviations are obtained for ΔH° . To circumvent either incomplete or too fast protein saturation an amount of 70% to 90% over-titration is advisable. As a rough estimate the shape of the thermogram should be analyzed. If stoichiometry is passed within one injection, the concentration is likely too high, if several injections (4–5 injections) are required to meet stoichiometry, the syringe concentration is too low and sufficient saturation will hardly be accomplished. Remarkably, the measurements at high saturation levels of over 90% show comparable results for ΔG° (Table 2) and they are in good accordance with the fluorescence-based assay results (Table 1). This finding suggests that the latter protocol gives more reliable ΔG° estimations for the fragments.

As important insight the present analysis shows, however, that the binding enthalpy of weak binding ligands measured by different displacement experiments may deviate depending on the actual properties of the reference ligand used for the titration. Important enough the relative differences between the binding enthalpies resulting from displacement titrations using deviating reference ligands are conserved.

In consequence, the relative data obtained by this strategy can be used to classify different fragments to exhibit a more enthalpic or entropic binding signature with respect to another fragment from the studied series.

4. Conclusions

Applying displacement titrations and direct titrations at low *c*-value, ITC can be used as a reliable technique to study low-affinity interactions as usually given for the binding of a fragment to a target protein. Reliable dissociation constants and thus affinities can be determined.

Some important aspects can be concluded from this study. First of all, the fragment must bind to a part of the protein binding pocket that overlaps with the binding pose region of the applied reference ligand. Secondly, the selected reference ligand must have a significant higher or lower binding enthalpy so that a heat difference signal can be recorded for the fragment (Fig. 6). Furthermore, it has to be regarded that, as for any displacement titration, all errors affecting the parameter determinations of the reference ligand will add to the accuracy of the parameters obtained for the fragment. Finally, if no suitable reference ligand is available and the fragment binds enthalpically enough, low *c*-value titrations can be applied as an alternative. In this case, however, some anticipated knowledge about the expected binding affinity of the fragment must be available to estimate the required excess concentration of the fragment at the end of the titration. In addition, the stoichiometry of the binding event must be arbitrarily fixed to an assumed value which may be in some cases questionable. This is in particular the case for weak binding fragments accommodated in large protein binding pockets. Nonetheless, as long as these conditions are regarded, displacement titrations as well as low *c*-value titrations are in convincing agreement to determine the binding affinities of fragments particularly if it is possible to achieve a concentration of the fragment in the sample cell at the end of the titration that exceeds the K_D value by a factor of 2–10 which corresponds to a saturation of 70 to 90%.

To our experience solubility of the fragment and the protein are the most crucial issues in low *c*-value titrations because the required high concentrations of the fragment to be studied in the injection syringe must match or even exceed the final sample cell concentrations

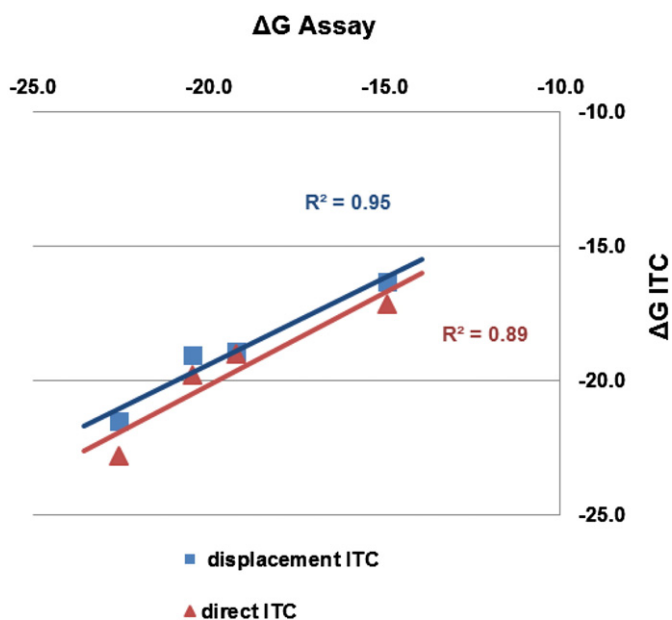


Fig. 6. The binding affinities expressed by $\Delta G = -RT \ln K$, are plotted against each other in kJ/mol to assess their mutual correlation, where K reflects either the thermodynamic dissociation constant K_D (displacement ITC and direct ITC) or the enzyme kinetic binding constant K_i (biochemical assay) of fragments 1–4.

with respect to the fragment's K_D value. Only then data with good signal-to-noise level can be recorded. Furthermore, to estimate the required concentration of the fragment, a crude idea of the fragment's K_D must be available from an independent experiment.

Measured binding enthalpies should not be compared quantitatively across different experimental conditions, but only relative to each other by using one carefully selected measurement protocol. Remarkably, different reference ligands used for the displacement of pre-incubated fragments reveal deviating enthalpic signals. Most likely these differences can be traced back to effects deviating from additivity. They possibly involve changes in the residual solvation structures and protein dynamics of the regarded protein–ligand complexes. Nonetheless, considering the relative enthalpy differences across the different displacement experiments seems to reveal a consistent picture, which subsequently allows to characterize the studied fragments relative to one another. Furthermore, detailed interpretation of the enthalpic signature requires a comparison of the corresponding crystal structures which will be performed in a subsequent contribution. Usually this information is required to select fragments as superior enthalpy-dominated candidates for further development.

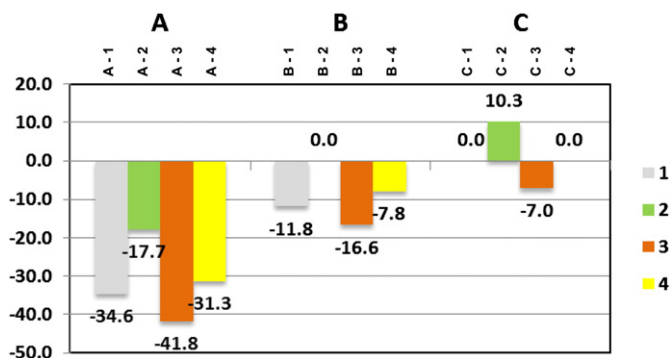


Fig. 7. Binding enthalpy differences $\Delta\Delta H$ between reference ligands **A**, **B**, **C** and fragment 1–4 are plotted in kJ/mol. In three cases no measurable enthalpy difference could be detected (0.0) as the heat signal produced by the displacement of the fragment is virtually compensated by the signal of the binding of the reference ligand.

5. Experimental section/materials & methods

5.1. ITC

ITC experiments were performed using an ITC200™ system from GE Healthcare, Northampton, MA, USA.

Thrombin was obtained from CSL Behring (Marburg, Germany) and purified from Beriplast® as one batch for the entire experimental series. Thrombin was extracted by dialysis using an experimental buffer of 50 mM TSPP, 100 mM NaCl, 0.1% polyethylene glycol 8000, and pH 7.8. Subsequently, the protein could be used for all titration experiments. The protein concentration was measured by absorbance at 280 nm using a NanoDrop 2000c Spectrophotometer from Thermo Scientific.

All ITC experiments were started at 25 °C with a reference power of 5 kcal/s after a stable baseline had been achieved. The pre-titration delay was set to 300 s. For direct titrations ligand injections of 0.3 μL (to prevent artifacts arising from small syringe leakages or air in the syringe) were followed by 19 to 27 injections of 1.5–2.0 μL with at least 180 s interval between each injection.

For displacement experiments, fragments from 500 mM DMSO stock solutions were used directly to saturate the thrombin solution (42 μM). Subsequently the DMSO concentration in all solutions was adjusted to 3%. All titrations were performed at least in duplicate.

In case of fragment **1** only a saturation concentration close to its K_D for thrombin could be achieved due to poor solubility in the buffer. For fragments **2** to **4** a final concentration of five to ten-times larger than the K_D for thrombin binding could be achieved and according to the Eq. (1) corresponds to a 50% to 91% saturation (D_{sat}).

$$[\text{fragment}]_{\text{cell}} = \frac{D_{\text{sat}} [\text{Protein}] - [\text{Protein}] - K_D \text{ fragment}}{1 - \frac{1}{D_{\text{sat}}}} \quad (1)$$

As supporting information we provide an Excel sheet to calculate the degree of saturation, according to Eq. (1) depicted below (Fig. 9) for ligands with affinities from 0.1 mM to 2 mM the typical range found for fragments. Subsequently, the high-affinity ligands **A**, **B**, **C** (0.5 mM from 50 mM DMSO stock solution) were added to the thrombin–fragment complex using 22 to 27 injections of 1.3 to 1.5 μL. Data were integrated using the program Nitpic 1.0.0 [29] which provides an automatic baseline determination and peak integration by peak-shape analysis, which is extremely valuable when dealing with data showing low signal-to-noise levels.

Isotherm fitting was conducted with the program SEDPHAT 10.58d [30]. The first data points were excluded from data analysis. K_a and ΔH for the fragments have been calculated using Eqs. (2) and (3), adapted from Zhang et al. [14]

$$K_{\text{fragment}} = \left(\frac{K_{\text{reference ligand}} - 1}{K_{\text{displacement titration}}} \right) \frac{1}{[\text{fragment}]_{\text{cell}}} \quad (2)$$

$$\Delta H^{\circ}_{\text{fragment}} = \left(\Delta H^{\circ}_{\text{reference ligand}} - \Delta H^{\circ}_{\text{displacement titration}} \right) \left(1 + \frac{1}{K_{\text{fragment}} [\text{fragment}]_{\text{cell}}} \right) \quad (3)$$

5.2. Bioassay

Kinetic inhibition of human thrombin (from Beriplast®, CSL Behring, Marburg, Germany) was determined photometrically for the reference ligands at 405 nm using the chromogenic substrate Pefachrom tPa (Loxo GmbH, Dossenheim, Germany) as previously described [31] under the following conditions: 50 mM Tris–HCl, pH 7.4, 154 mM NaCl, 5% DMSO, 0.1% polyethylene glycol 8000 at 25 °C using different concentrations of substrate and inhibitor. K_i values with $n \geq 3$ were determined as described by Dixon [32].

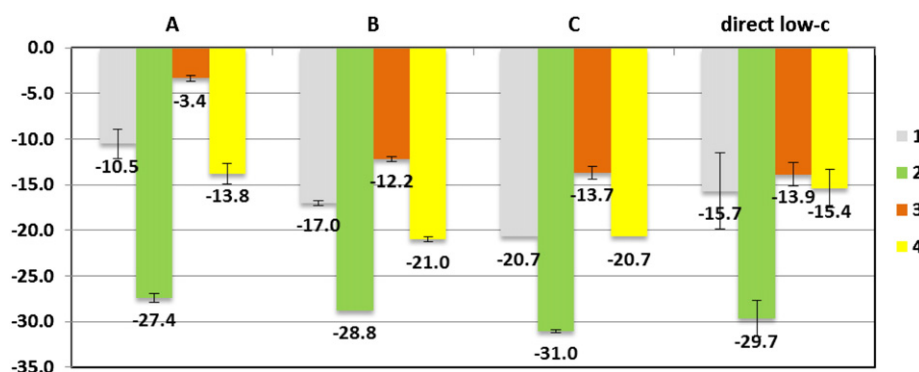


Fig. 8. Direct comparison of the enthalpic data across the fragment series, 1 (white), 2 (green), 3 (orange) and 4 (yellow) plotted in kJ/mol for displacement titrations with reference ligands A, B, C and direct low-c value titrations.

Thrombin fragments were characterized by a more sensitive fluorogenic assay. Kinetic data were obtained using Tos-Gly-Pro-Arg-AMC (tosyl-Gly-Pro-Arg-aminomethylcoumarin) as the fluorogenic substrate [33] with a Safire II plate reader (Tecan, Switzerland, ex = 380 nm, em = 460 nm). The experimental buffer contained 50 mM Tris-HCl, 154 mM NaCl, 0.1% polyethylene glycol 8000 and 5% DMSO at pH 7.4. The K_m of the substrate ($5.7 \pm 0.4 \mu\text{M}$) was measured at eleven different substrate concentrations and the resulting curve was analyzed using GraFit 4 (Erithacus Software Limited, Staines, UK). Substrate cleavage was measured by monitoring the change in fluorescence across a dilution series of at least ten inhibitor concentrations ($6.25\text{--}0.01 \text{ mM}$) at $1 \mu\text{M}$ substrate over 600 s. The fluorescence signal was plotted versus time and by linear regression the reaction rates were calculated. The reaction rates were plotted against the respective inhibitor concentration and the resulting curve was fitted with ORIGIN software using Michaelis-Menten kinetics. All measurements were performed at least in triplicate.

Acknowledgement

The present study was kindly supported by the ERC Advanced Grant no. 268145-DrugProfilBind awarded to GK. We kindly acknowledge CSL Behring (Marburg) for supplying us with generous amounts of human

thrombin from the production of Beriplast®. Helpful discussions by Dr. Adam Biela and Matthias Groh (Univ. Marburg) in the beginning of this project are gratefully appreciated.

Appendix A. Supplementary data

Supplementary data to this article can be found online at <http://dx.doi.org/10.1016/j.bbagen.2014.12.007>.

References

- [1] J.E. Ladbury, G. Klebe, E. Freire, Adding calorimetric data to decision making in lead discovery: a hot tip, *Nat. Rev. Drug Discov.* 9 (2010) 23–27.
- [2] E. Freire, A thermodynamic approach to the affinity optimization of drug candidates, *Chem. Biol. Drug Des.* 74 (2009) 468–472.
- [3] J.B. Chaires, Calorimetry and thermodynamics in drug design, *Annu. Rev. Biophys.* 37 (2008) 135–151.
- [4] T.S.G. Olsson, M.A. Williams, W.R. Pitt, J.E. Ladbury, The thermodynamics of protein–ligand interaction and solvation: insights for ligand design, *J. Mol. Biol.* 384 (2008) 1002–1017.
- [5] A. Glas, D. Bier, G. Hahne, C. Rademacher, C. Ottmann, T.N. Grossmann, Constrained peptides with target-adapted cross-links as inhibitors of a pathogenic protein–protein interaction, *Angew. Chem. Int. Ed. Engl.* 53 (2014) 2489–2493.
- [6] G.E. de Kloe, D. Bailey, R. Leurs, I.J.P. de Esch, Transforming fragments into candidates: small becomes big in medicinal chemistry, *Drug Discov. Today* 14 (2009) 630–646.
- [7] G.G. Ferenczy, G.M. Keserü, Thermodynamics of fragment binding, *J. Chem. Inf. Model.* 52 (2012) 1039–1045.
- [8] G.G. Ferenczy, G.M. Keserü, How are fragments optimized? A retrospective analysis of 145 fragment optimizations, *J. Med. Chem.* 56 (2013) 2478–2486.
- [9] V. Borsi, V. Calderone, M. Fragai, C. Luchinat, N. Sarti, Entropic contribution to the linking coefficient in fragment based drug design: a case study, *J. Med. Chem.* 53 (2010) 4285–4289.
- [10] S.F. Martin, J.H. Clements, Correlating structure and energetics in protein–ligand interactions: paradigms and paradoxes, *Annu. Rev. Biochem.* 82 (2013) 267–293.
- [11] M. Congreve, G. Chessari, D. Tisi, A.J. Woodhead, Recent developments in fragment-based drug discovery, *J. Med. Chem.* 51 (2008) 3661–3680.
- [12] J.D. Taylor, P.J. Gilbert, M.A. Williams, W.R. Pitt, J.E. Ladbury, Identification of novel fragment compounds targeted against the pY pocket of v-Src SH2 by computational and NMR screening and thermodynamic evaluation, *Proteins* 67 (2007) 981–990.
- [13] D.C. Rees, M. Congreve, C.W. Murray, R. Carr, Fragment-based lead discovery, *Nat. Rev. Drug Discov.* 3 (2004) 660–672.
- [14] Y.L. Zhang, Z.Y. Zhang, Low-affinity binding determined by titration calorimetry using a high-affinity coupling ligand: a thermodynamic study of ligand binding to protein tyrosine phosphatase 1B, *Anal. Biochem.* 261 (1998) 139–148.
- [15] W.G. Eisert, N. Huel, J. Stangier, W. Wienen, A. Clemens, J. van Ryn, Dabigatran: an oral novel potent reversible nonpeptide inhibitor of thrombin, *Arterioscler. Thromb. Vasc. Biol.* 30 (2010) 1885–1889.
- [16] M. Fricke, Diploma Thesis, FU Berlin, Germany, (2013)
- [17] K. Hilpert, J. Ackermann, D.W. Banner, A. Gast, K. Gubernator, P. Hadváry, L. Labler, K. Müller, G. Schmid, T.B. Tschopp, Design and synthesis of potent and highly selective thrombin inhibitors, *J. Med. Chem.* 37 (1994) 3889–3901.
- [18] T. Steinmetzer, J. Stürzebecher, Progress in the development of synthetic thrombin inhibitors as new orally active anticoagulants, *Curr. Med. Chem.* 11 (2004) 2297–2321.
- [19] M. T. Khayat PhD Thesis, University at Buffalo, USA, (2013)
- [20] B. Baum, M. Mohamed, M. Zayed, C. Gerlach, A. Heine, D. Hangauer, G. Klebe, More than a simple lipophilic contact: a detailed thermodynamic analysis of nonbasic residues in the S1 pocket of thrombin, *J. Mol. Biol.* 390 (2009) 56–69.

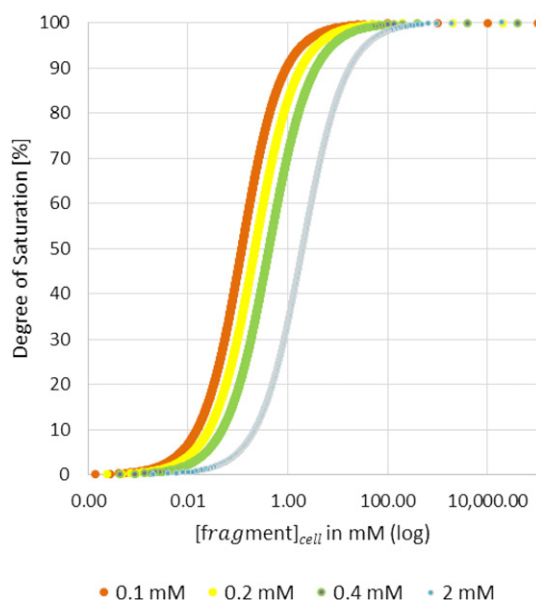


Fig. 9. Degree of saturation (D_{sat}) is plotted against ligand concentration in the sample cell ($[\text{fragment}]_{\text{cell}}$) on logarithmic scale for affinities from 0.1 mM to 2 mM.

- [21] B. Baum, L. Muley, A. Heine, M. Smolinski, D. Hangauer, G. Klebe, Think twice: understanding the high potency of bis(phenyl)methane inhibitors of thrombin, *J. Mol. Biol.* 391 (2009) 552–564.
- [22] A. Biela, F. Sielaff, F. Terwesten, A. Heine, T. Steinmetzer, G. Klebe, Ligand binding stepwise disrupts water network in thrombin: enthalpic and entropic changes reveal classical hydrophobic effect, *J. Med. Chem.* 55 (2012) 6094–6110.
- [23] T. Wiseman, S. Williston, J.F. Brandts, L.N. Lin, Rapid measurement of binding constants and heats of binding using a new titration calorimeter, *Anal. Biochem.* 179 (1989) 131–137.
- [24] W.B. Turnbull, A.H. Daranas, On the value of c : can low affinity systems be studied by isothermal titration calorimetry? *J. Am. Chem. Soc.* 125 (2003) 14859–14866.
- [25] W.B. Turnbull, B.L. Precious, S.W. Homans, Dissecting the cholera toxin-ganglioside GM1 interaction by isothermal titration calorimetry, *J. Am. Chem. Soc.* 126 (2004) 1047–1054.
- [26] W.B. Turnbull, Divided we fall? Studying low-affinity fragments of ligands by ITC, GE Application Note (2011).
- [27] J. Broecker, C. Vargas, S. Keller, Revisiting the optimal c -value for isothermal titration calorimetry, *Anal. Biochem.* 418 (2011) 307–309.
- [28] J. Tellinghuisen, Isothermal titration calorimetry at very low c , *Anal. Biochem.* 373 (2008) 395–397.
- [29] S. Keller, C. Vargas, H. Zhao, G. Piszczek, C.A. Brautigam, P. Schuck, High-precision isothermal titration calorimetry with automated peak-shape analysis, *Anal. Chem.* 84 (2012) 5066–5073.
- [30] J.C. Houtman, P.H. Brown, B. Bowden, H. Yamaguchi, E. Appella, L.E. Samelson, P. Schuck, Studying multisite binary and ternary protein interactions by global analysis of isothermal titration calorimetry data in SEDPHAT: application to adaptor protein complexes in cell signaling, *Protein Sci.* 16 (2007) 30–42.
- [31] J. Stürzebecher, U. Stürzebecher, H. Vieweg, G. Wagner, J. Hauptmann, F. Markwardt, Synthetic inhibitors of bovine factor Xa and thrombin comparison of their anticoagulant efficiency, *Thromb. Res.* 54 (1989) 245–252.
- [32] M. Dixon, The graphical determination of K_m and K_i , *Biochem. J.* 129 (1972) 197–202.
- [33] M.J. Bennett, S.I. Blaber, I.A. Scarisbrick, P. Dhanarajan, S.M. Thompson, M. Blaber, Crystal structure and biochemical characterization of human kallikrein 6 reveals that a trypsin-like kallikrein is expressed in the central nervous system, *J. Biol. Chem.* 277 (2002) 24562–24570.